

Supporting information

Effect of Coexisting TiO₂ Powder on Ionic Conduction of Highly Concentrated LiTFSA Aqueous Electrolyte (20.5 mol kg⁻¹)

Jingchao XU,^{a, §} Hideshi MAKI,^{a, §§} Hiro MINAMIMOTO,^{a, §§} and Minoru MIZUHATA,^{a, *, §§}

^a *Department of Chemical Science and Engineering, Graduate School of Engineering, Kobe University, 1-1 Rokkodai-cho, Nada-ku, Kobe 657-8501, Japan*

* *Corresponding author: mizuhata@kobe-u.ac.jp*

† A part of this paper has been presented in the 64th Battery Symposium in Japan in 2023 (Presentation #2G04) and the 2023 ECSJ Fall Meeting (Presentation #P16)

§ ECSJ Student Member

§§ ECSJ Active Member

ORCID J. Xu: 0009-0007-3697-0497

M. Maki: 0000-0002-8960-4833

H. Minamimoto: 0000-0002-2360-577X

M. Mizuhata: 0000-0002-4496-2215

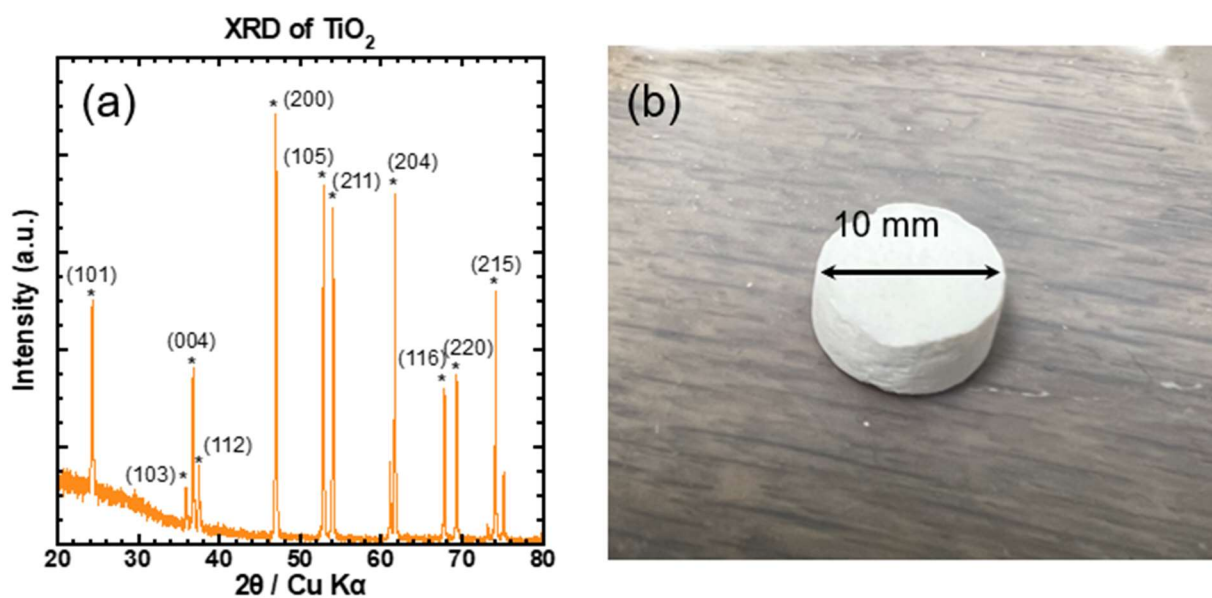


Figure S1. (a) XRD results of anatase TiO₂; (b) Schematic diagram of the sample obtained by compressing a homogeneous mixture of TiO₂ powder and liquid phase in a mold at 5 MPa for 30 minutes, with a sample diameter of 10 mm.

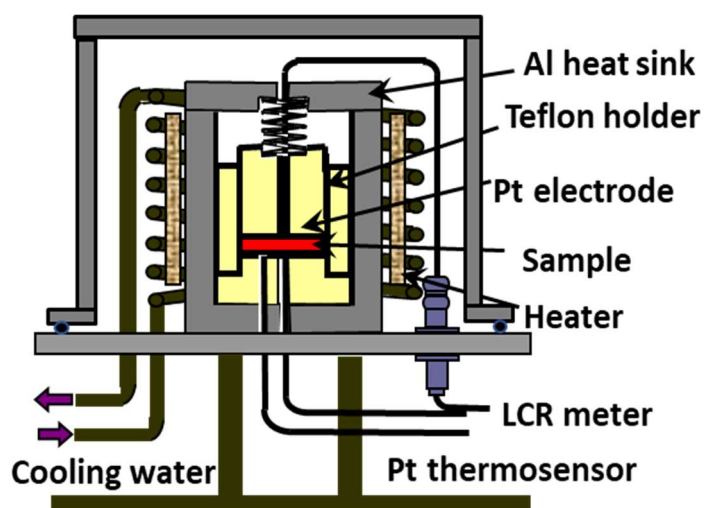
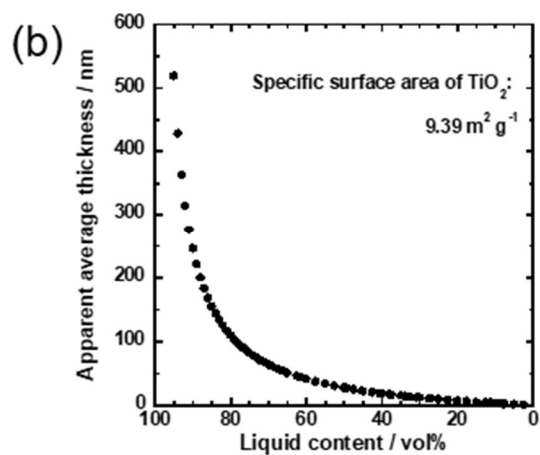
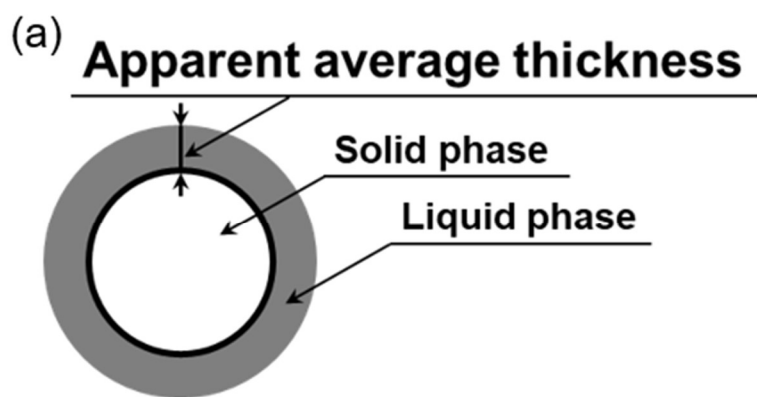


Figure S2. Schematic diagram of the cell used for testing solid-liquid coexistence samples. The cylindrical sample has a platinum electrode at both the top and bottom, maintained in full contact with the sample through springs and applied constant external force. The internal temperature of the cell is monitored in real time using a thermometer, and the temperature is controlled by a heater. Once the thermometer reading reaches the target temperature, it is maintained for 5 minutes to ensure that the sample temperature is consistent with the cell temperature.



$$\text{Apparent average thickness} = \frac{\text{Total volume of liquid phase}}{\text{Total surface area of solid phase}}$$

Figure. S3. (a) Schematic drawing of the solid-liquid coexistence system; (b) Relationship between average thickness of liquid phase and volume fraction of liquid phase.

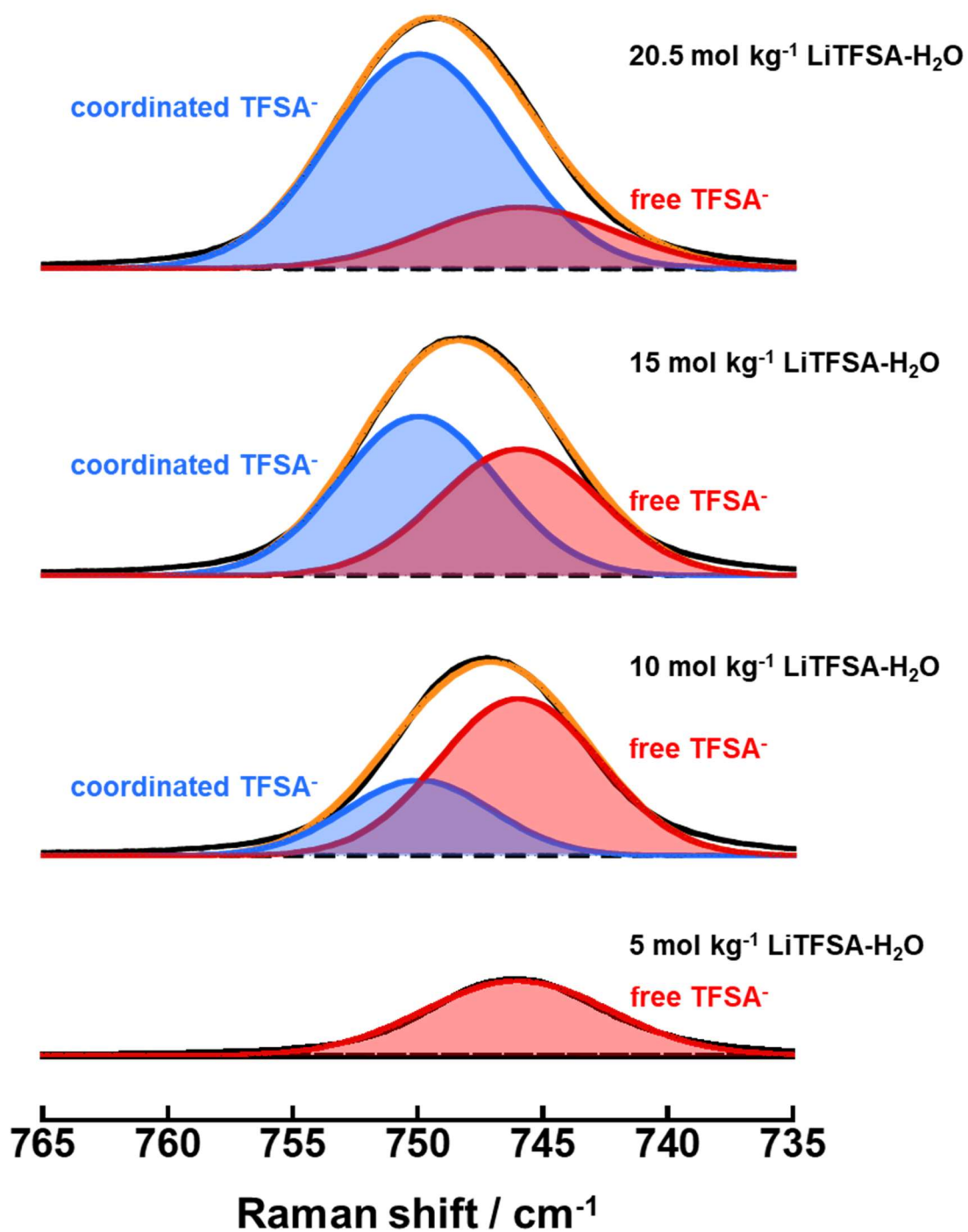


Figure S4. Deconvoluted bands of the Raman spectra of the S-N-S bending mode in TFSA⁻ anion in different concentrations of LiTFSA aqueous solutions. The red band represents free TFSA⁻ without interaction of Li⁺, and the blue band represents TFSA⁻ interacted with Li⁺ ion.

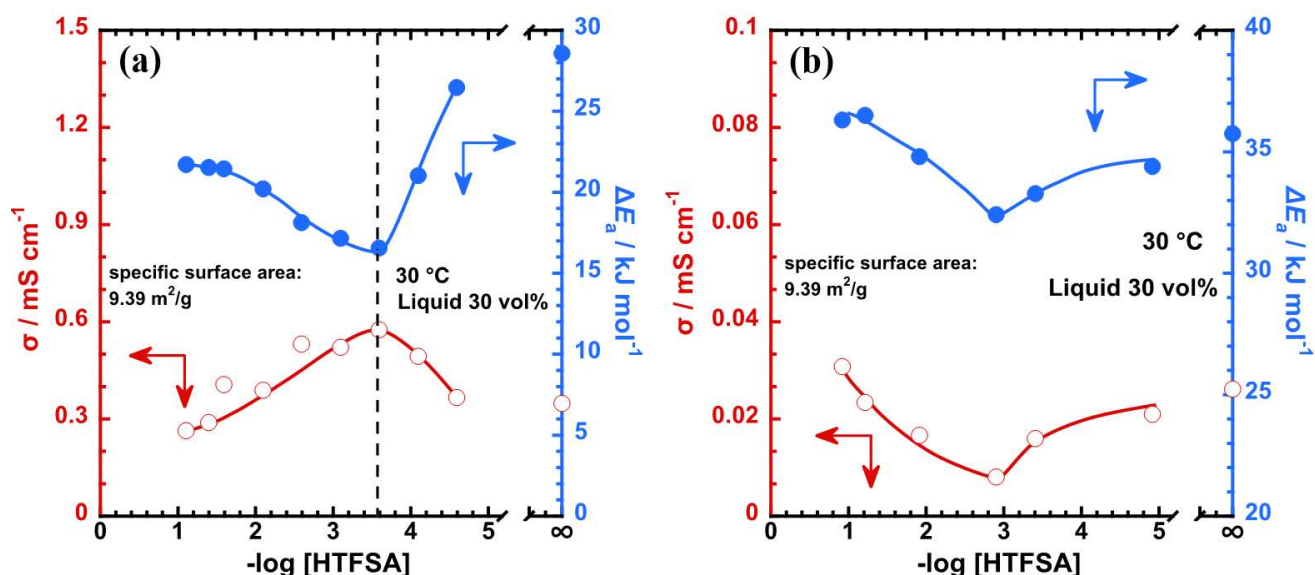


Figure S5. Results of changes in conductivity (red) and activation energies (blue) with the amount of HTFSA added to LiTFSA aqueous electrolyte at a liquid phase volume fraction of 30 vol%. (a) 1 mol kg^{-1} , (b) 20.5 mol kg^{-1} . The solid-liquid coexistence samples with a liquid phase volume fraction of 30 vol% were prepared by adjusting the pH of the solution with the addition of HTFSA to the aqueous electrolyte of LiTFSA and mixing the pH-adjusted aqueous solution with TiO_2 powder. The horizontal axis indicates the logarithmic opposite of the HTFSA added to the bulk solution. Results for conductivity and activation energies without HTFSA addition are shown at “ ∞ ” on the right side of the graph. The pH of the aqueous electrolytes of LiTFSA for bulk 1 mol kg^{-1} and 20.5 mol kg^{-1} without pH adjustment were 6.3 and 2.4, respectively, and the pzc of TiO_2 was ca. 6.

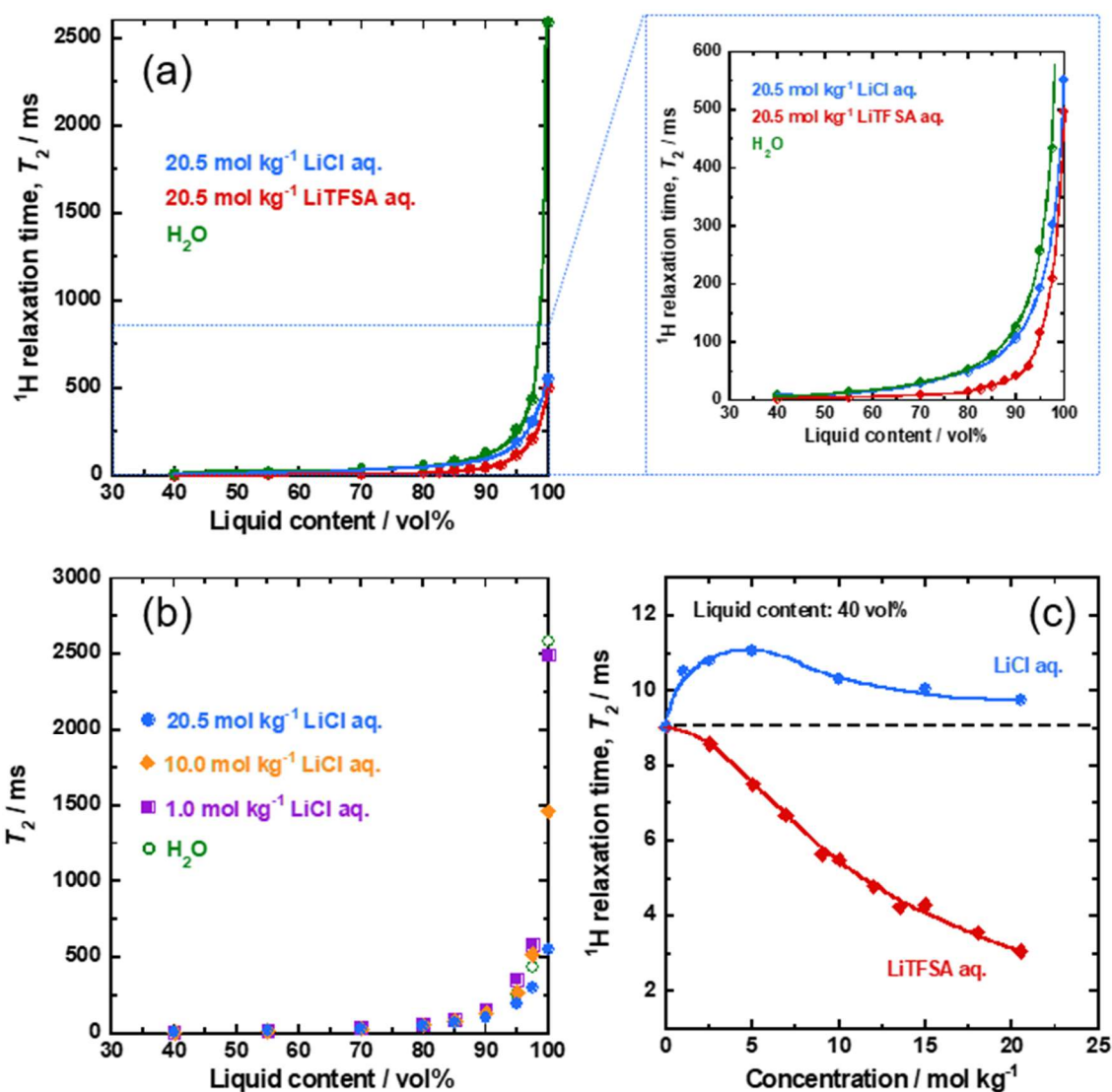


Figure S6. T_2 relaxation times of hydrogen nuclei in water molecules within the $\text{TiO}_2/\text{LiCl-H}_2\text{O}$ and $\text{LiTFSA-H}_2\text{O}$ solid-liquid coexistence systems. (a) The relationship between the T_2 relaxation time of hydrogen nuclei in water molecules and liquid phase volume fraction in the 20.5 mol kg⁻¹ $\text{LiCl-H}_2\text{O}$ (blue), 20.5 mol kg⁻¹ $\text{LiTFSA-H}_2\text{O}$ (red), and pure water (green) / TiO_2 coexistence systems. (b) Variation of T_2 relaxation time of hydrogen nuclei in different concentrations of $\text{TiO}_2/\text{LiCl-H}_2\text{O}$ solid-liquid coexistence systems with liquid phase volume fraction. (c) The T_2 relaxation times of water molecules (H) in 20.5 mol kg⁻¹ $\text{LiCl-H}_2\text{O}$ (blue) and 20.5 mol kg⁻¹ $\text{LiTFSA-H}_2\text{O}$ (red) as a function of electrolyte concentration at a liquid phase volume fraction of 40 vol%.